crystals

MDPI

Article

Effect of Silver Vanadate Nanowires Addition on Structural and Morphological Properties of Dental Porcelain Prepared from Economic Raw Materials

Badr Eddine Sakhkhane [1], Marieta Mureșan-Pop [2,3], Lucian Barbu-Tudoran [4,5], Tamás Lovász [6] and Liliana Bizo [1,2,*]

[1] Department of Chemical Engineering, Faculty of Chemistry and Chemical Engineering, Babeș-Bolyai University, 11 Arany Janos Street, RO-400028 Cluj-Napoca, Romania; badreddinecb@gmail.com
[2] Institute for Interdisciplinary Research on Bio-Nano-Sciences, Babeș-Bolyai University, 42 Treboniu Laurian Street, RO-400271 Cluj-Napoca, Romania; marieta.muresan@ubbcluj.ro
[3] INSPIRE Research Platform, Babeș-Bolyai University, 11 Arany Janos Street, RO-400028 Cluj-Napoca, Romania
[4] Electron Microscopy Center, Faculty of Biology and Geology, Babeș-Bolyai University, 5-7 Clinicilor Street, RO-400006 Cluj-Napoca, Romania; lucian.barbu@ubbcluj.ro
[5] Electron Microscopy Integrated Laboratory, National Institute for Research and Development of Isotopic and Molecular Technologies, 67-103 Donath Street, RO-400293 Cluj-Napoca, Romania
[6] Department of Chemistry and Chemical Engineering of Hungarian Line of Study, Faculty of Chemistry and Chemical Engineering, Babeș-Bolyai University, 11 Arany Janos Street, RO-400028 Cluj-Napoca, Romania; tamas.lovasz@ubbcluj.ro
* Correspondence: liliana.bizo@ubbcluj.ro; Tel.: +40-264-593833

Abstract: In addition to many materials, silver vanadate ($AgVO_3$) has gained interest due to its antimicrobial properties, which opens up the potential for use as an antibacterial agent for biomedical applications. This work aimed to study the effect of $AgVO_3$ addition on the structural and morphological properties of a developed dental porcelain (DP) prepared from natural raw materials. $AgVO_3$ nanowires, prepared by the coprecipitation method, were added in different amounts (1, 3, and 5 wt.%) to a DP mass with the initial composition of 80 wt.% feldspar, 15 wt.% quartz, and 5 wt.% kaolin, obtained by sintering the mixture at 1300 °C. The structural and morphological properties of $AgVO_3$ and DP were investigated by X-ray powder diffraction (XRPD), Fourier transform infrared spectroscopy (FTIR), scanning electron microscopy/energy-dispersive X-ray spectroscopy (SEM/EDS), and transmission electron microscopy (TEM). The results showed the formation of α-$AgVO_3$ nanowires coated with semispherical metallic silver nanoparticles. Moreover, α-$AgVO_3$ additions do not influence the structural and morphological properties of DP, with the presence of Ag and V clearly identified in the DP with the α-$AgVO_3$ addition. Our findings highlight the potential of this novel material for use in various dental applications. Future studies need to establish the antibacterial properties of the prepared dental material.

Keywords: biomaterials; silver vanadate nanowires; dental porcelain; structural properties; morphological properties

Citation: Sakhkhane, B.E.; Mureșan-Pop, M.; Barbu-Tudoran, L.; Lovász, T.; Bizo, L. Effect of Silver Vanadate Nanowires Addition on Structural and Morphological Properties of Dental Porcelain Prepared from Economic Raw Materials. *Crystals* **2024**, *14*, 616. https://doi.org/10.3390/cryst14070616

Academic Editor: Yan Zhang

Received: 31 May 2024
Revised: 23 June 2024
Accepted: 30 June 2024
Published: 3 July 2024

1. Introduction

The use of biomaterials is crucial in modern medicine, as they could be applied in restoring function and promoting healing after illness or injury. Biomaterials can either be natural or synthetic, and are utilized to reinforce, improve, or substitute damaged biological tissue or functions [1,2]. Today, the field of biomaterials has been greatly influenced by advances in many areas of biotechnology and science [3]. Biomaterials, which are utilized in the field of biomedical engineering, encompass a broad spectrum of substances, including metals (such as titanium or stainless steel), ceramics (such as alumina or zirconia), plastics

(such as polyethylene or polymethyl methacrylate), glass, living cells, and tissue. These constituent materials are versatile and can be processed and manipulated into various intricate forms, including molded components, machined parts, specialized coatings, advanced fibers, thin films, foams with specific properties, and textiles designed for biomedical applications. The applications of these biomaterials are diverse, serving in the development and production of a wide range of biomedical products and devices [1]. Examples of such products include but are not limited to artificial heart valves, sophisticated hip joint replacements, biocompatible dental implants, and innovative contact lenses [4].

Ceramics are frequently used as biomaterials in dentistry, especially as dental restorative materials such as crowns, bridges, and false teeth. The materials used for this purpose are referred to as bioceramics [5]. Bioceramics can be defined as inorganic, non-metallic, and biocompatible materials characterized by their chemical stability, non-corrosiveness, and favorable interaction with organic tissues [6]. This category includes zirconia and alumina, coatings and composites, hydroxyapatite and resorbable calcium phosphates, and bioactive and radiotherapy glasses [7]. The clinical use of bioceramics in dentistry started in the late eighteenth century with the use of porcelain in crowns [8].

Dental porcelain distinguishes itself from traditional ceramics primarily due to its firing methods, making it more appropriate for dental restorations [9]. Along with enhanced aesthetic qualities such as color, intensity, and translucency, dental porcelain materials also offer remarkable biocompatibility and longevity as their primary benefits [10]. Dental porcelain is a mixture of kaolin, feldspar, and quartz [11], and refers to a specific compositional range of ceramic materials obtained by mixing the raw materials in an appropriate proportion and fired at a high temperature [12–15]. Kaolin, a hydrated aluminum silicate, with kaolinite ($Al_2O_3 \cdot 2SiO_2 \cdot 2H_2O$) as the main constituent, serves as a binding agent. Quartz (SiO_2) remains unchanged during the firing process, contributing to the material's strength. The feldspars present are mixtures of sodium aluminosilicate ($6SiO_2 \cdot Al_2O_3 \cdot Na_2O$), commonly referred to as albite, and potassium aluminosilicate ($6SiO_2 \cdot Al_2O_3 \cdot K_2O$) [15]. The earliest attempts to enhance dental porcelain involved the incorporation of strengthening oxide particles, like aluminum oxide and zirconium oxide, in the base porcelain. Recently, due to advancements in computer-aided design and manufacturing (CAD/CAM) technology and the introduction of glass-infiltrated ceramics, it has become possible to use pure alumina and PSZ (partially stabilized zirconia) [16]. Dental porcelain powders could also be mixed with additional metal oxides such as MgO, ZnO, $AgVO_3$, etc., which bring antibacterial properties, resistance to thermal shock, and could offer a wide range of colors [14].

The antibacterial qualities of silver have been recognized for centuries [17]. Lately, silver nanoparticles (AgNPs), due to the antimicrobial properties exhibited, have attracted considerable interest, which opens up the potential for medical applications [18–20]. It is considered a promising compound for use in dentistry. However, their commercial use is still in the early stages, with only a few products on the market currently incorporating AgNPs into their composition [21]. In addition to numerous silver-based materials, which are considered to be promising candidates for antimicrobial agents, beta-silver vanadate (β-$AgVO_3$) has demonstrated significant potential as an antimicrobial agent. Its effectiveness is particularly notable when in the form of nanorods, nanowires, or nanotubes, and stands out due to its considerable stability and the ability to adjust its properties by modifying its composition, size, form, crystal structure, and surface characteristics [22,23]. Holtz et al. demonstrated that the antibacterial properties of β-$AgVO_3$ are attributed to the release of silver and vanadium ions by the nanomaterial upon interaction with bacteria [22]. Many researchers have indicated that incorporating β-$AgVO_3$ into acrylic resins or dental porcelain inhibited bacterial growth and exhibited antibacterial effects against various bacteria, such as *Streptococcus mutans*, *Staphylococcus aureus*, and *Pseudomonas aeruginosa* [18,19,24–28]. Apart from the stable phase β-$AgVO_3$, the metastable phase α-$AgVO_3$ is formed instantly below the melting point when slowly cooled or rapidly frozen [27]. Even if few studies have been found to analyze the antibacterial activity of α-$AgVO_3$, the research of Alves da

Silva Pimentel et al. has suggested its antimicrobial potential against *C. albicans*, exhibiting fungicidal and fungistatic activity [29]. In addition, it was shown that α-$AgVO_3$ microcrystals are not cytotoxic against keratinocyte cells, regardless of morphological variations. This emphasizes that this novel and safe antimicrobial compound could be used in biomedical and dental applications [29]. However, many excellent antimicrobial agents may also cause undesirable toxicity to animals and plants. Consequently, toxicity analyses are crucial for the safe use of these materials in dentistry [26].

Many research groups have successfully developed nanostructured silver vanadate decorated with silver nanoparticles (β-$AgVO_3$), which has been extensively studied in various dental materials. The material effectively stabilizes silver nanoparticles (AgNPs), preventing agglomeration and ensuring the continuous release of antimicrobial silver ions. In a recent study, Ferreira et al. analyzed the hardness, roughness, and color change of pit and fissure sealants from two commercial brands, Fluroshield™ and Ultraseal XT™. These sealants were enhanced with nanostructured silver vanadate nanomaterial decorated with silver nanoparticles (β-$AgVO_3$) at concentrations of 0%, 2.5%, and 5%, respectively [30]. Their findings demonstrated that the addition of 2.5% and 5% β-$AgVO_3$ in pit and fissure sealants induced changes in the roughness of Ultraseal XT™, while maintaining the microhardness of both sealants. Furthermore, the Fluroshield™ underwent a color shift within acceptable clinical limits [30]. To evaluate the mechanical and biological properties of a denture adhesive (Ultra Corega Cream-UCCA) incorporating nanostructured silver vanadate ($AgVO_3$), Alvim et al. used specimens in poly(methyl methacrylate) (PMMA), which were treated with UCCA denture adhesive, with or without $AgVO_3$ [31]. The study involved the use of poly(methyl methacrylate (PMMA) specimens treated with the denture adhesive, both with and without the addition of $AgVO_3$ [31]. Their findings revealed that the combination of denture adhesives with $AgVO_3$ not only demonstrated antimicrobial effects but also exhibited superior adhesive strength, all without causing any cytotoxic effects. These results highlight the potential of $AgVO_3$ to enhance denture adhesives with implications for both oral health and overall well-being.

In the last few years, significant efforts have been made to produce $AgVO_3$ with various structures. The fabrication of specific nanostructures, including 0D, 1D, 2D, and 3D nanomaterials, has been pursued due to their unique size- and/or shape-dependent physicochemical properties [28]. In the field of dentistry, nanostructured β-$AgVO_3$ decorated with AgNPs has emerged as a promising additive for acrylic resins to enhance dental applications. This material possesses an excellent antimicrobial property, as the silver and vanadium elements can act synergistically against the main pathogenic microorganisms found in the oral cavity [22]. Ferreira et al. demonstrated that the addition of β-$AgVO_3$ in dental porcelain shows antimicrobial efficacy across all concentrations (2.5%, 5%, and 10%), while not affecting the Vickers microhardness [19]. In a related study, Kreve et al. indicated that the integration of β-$AgVO_3$ into a soft denture liner exhibited bactericidal activity against *P. aeruginosa*, *E. faecalis*, and *C. albicans*, and simultaneously enhanced the adhesion properties between the liner and the denture base material [32]. On the other hand, de Oliveira et al. demonstrated that α-$AgVO_3$ with different morphologies is subject to geometric constraints imposed by the crystal structure and is correlated with the relative surface energy values of each surface [33]. The study indicated that rod-shaped α-$AgVO_3$ crystals with prevalent (011) and (001) surfaces, characterized by low surface energies, exhibited enhanced antibacterial activity against MRSA bacteria. Finally, they concluded that the distinct morphologies of α-$AgVO_3$ crystals manifest varied chemical and physical properties, thereby rendering these materials interesting in different applications [33]. Briefly, the morphological properties of the silver vanadate strongly influenced the antibacterial activity of different dental materials, acting against a wide variety of bacteria from the oral cavity. Consequently, the aim of this work was to analyze the influence of different amounts of $AgVO_3$ addition on the structural and morphological properties of a new dental porcelain prepared from natural raw materials, which could produce an improved dental material.

2. Materials and Methods

2.1. Silver Vanadate Synthesis

The nanostructured silver vanadate was synthesized through a precipitation reaction, between silver nitrate (99.8% $AgNO_3$; VWR Chemicals, Singapore) and ammonium vanadate (99% NH_4VO_3; Thermo Scientific, Waltham, MA, USA) [22]. Firstly, 0.9736 g of NH_4VO_3 and 1.3569 g of $AgNO_3$ were dissolved in 200 mL of distilled water. The $AgNO_3$ solution was then added, drop by drop, to the NH_4VO_3 solution, while under constant agitation at 65 °C. The obtained precipitate with yellow coloration was washed with distilled water and absolute alcohol, filtered, and dried in a Fistreem vacuum oven for 10 h to obtain the silver vanadate powder.

2.2. Dental Porcelain Preparation

The raw materials used for porcelain preparation were quartz, feldspar, and kaolin. The composition of the produced porcelain was 80 wt.% feldspar, 15 wt.% quartz, and 5 wt.% kaolin. The raw material mixtures were wet-milled and homogenized in a laboratory planetary ball mill (Pulverisette 6, Fritsch, Germany) for 30 min at 250 rpm, to obtain the typical size distribution. Afterwards, the obtained mixtures were oven-dried at 105 °C for 12 h. After drying, the mixtures were uniaxial compacted into 2 g disc shapes using a Carver Inc., hydraulic press (Carver Inc., Wabash, IN, USA) at a pressure of ~0.5 tons, and subsequently sintered at 1300 °C for 1 h using an LHT 04/16 High-Temperature Furnace (Nabertherm GmbH, Lilienthal, Germany). The sintering process maintained a constant heating and cooling rate of 5 °C/min. Finally, the fired samples, in the form of powder, were subjected to different analyses.

2.3. Characterization Methods

Structural and morphological characterization of the prepared silver vanadate and dental porcelain was accomplished by X-ray powder diffraction (XRPD), Fourier transform infrared spectroscopy (FTIR), scanning electron microscopy/energy-dispersive spectroscopy (SEM/EDS), and transmission electron microscopy (TEM) analysis.

XRPD analysis was performed to investigate the structure of the samples using a Shimadzu XRD-6000 diffractometer (Shimadzu, Tokyo, Japan) operating at 40 kV, 30 mA, with Ni-filter and graphite monochromatic for CuKα (λ = 1.54060 Å). The diffraction patterns were recorded in the 2θ range of 10–80° at a scan speed of 2°/min.

Fourier transform infrared (FTIR) absorption spectra were recorded in KBr pellets with a Bruker Vector 22 FTIR spectrometer (Bruker, Karlsruhe, Germany). The measured samples were in the form of KBr pellets, measured in the range of 600 to 4000 cm^{-1}. The background spectrum of the KBr pellets was recorded under identical instrumental conditions and subtracted from each sample spectrum automatically. The data analysis was realized utilizing the Spectra Analysis software.

The materials' morphology was investigated using a HD-2700 (Hitachi, Tokyo, Japan) transmission electron microscope (TEM) equipped with a digital image recording system and an SU8230 (Hitachi, Tokyo, Japan) scanning electron microscope (SEM). The electron microscope was coupled with an Aztec X-Max 1160 EDX detector (Oxford Instruments, Abingdon, UK). The SEM/EDS images were acquired using 30 kV, 10 μA. To prepare the samples, the material was fixed with double-sided carbon tape, grounded with silver paste, and then sputter-coated with 10 nm of gold in an Argon environment.

3. Results and Discussion

3.1. Silver Vanadate Characterization

For the structural analysis of the $AgVO_3$ samples prepared by precipitation, they were measured by XRPD. From the reaction of the precursors used in the preparation, we expected a silver vanadate to form. As a result, the diffractogram was analyzed with the PDF database (JCPDS 29-1154). A perfect match of the diffraction peaks was not obtained. For this reason, it was simulated from the Crystallography Open Database

(COD, 1509498.cif), the codes corresponding to silver vanadate [34]. It was found that the simulated diffractogram perfectly overlaps the experimental diffractogram of our sample (Figure 1). The α-$AgVO_3$ monoclinic phase crystallizes in the C 2/c group, with the parameters of the elementary cell a = 10.437, b = 9.897, c = 5.532, α = 90, β = 99.69, and γ = 90. The perfect concordance of the diffraction peaks of the prepared sample with the phase from COD indicates the high purity of the obtained phase.

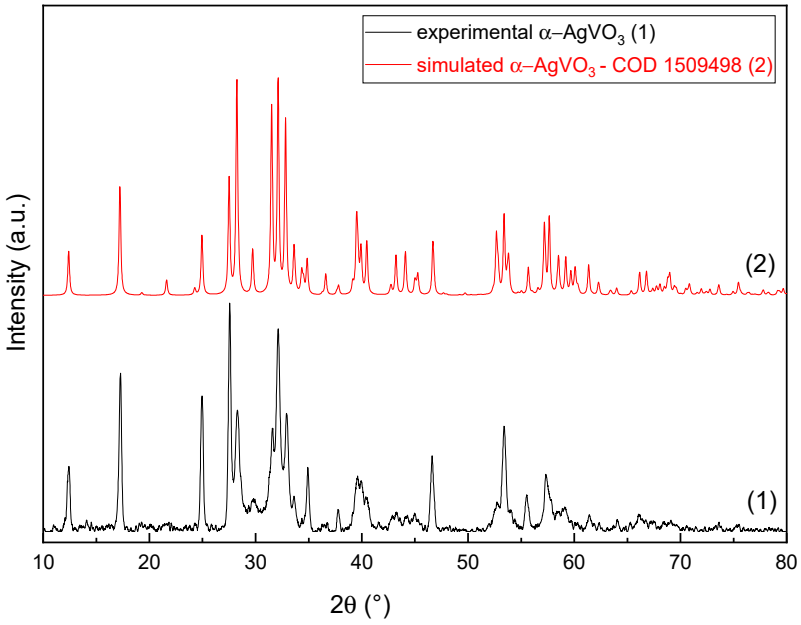

Figure 1. XRPD powder patterns of the α-$AgVO_3$ sample, experimental and simulated from COD database.

The FTIR absorption spectrum of the synthesized silver vanadate nanowires is displayed in Figure 2.

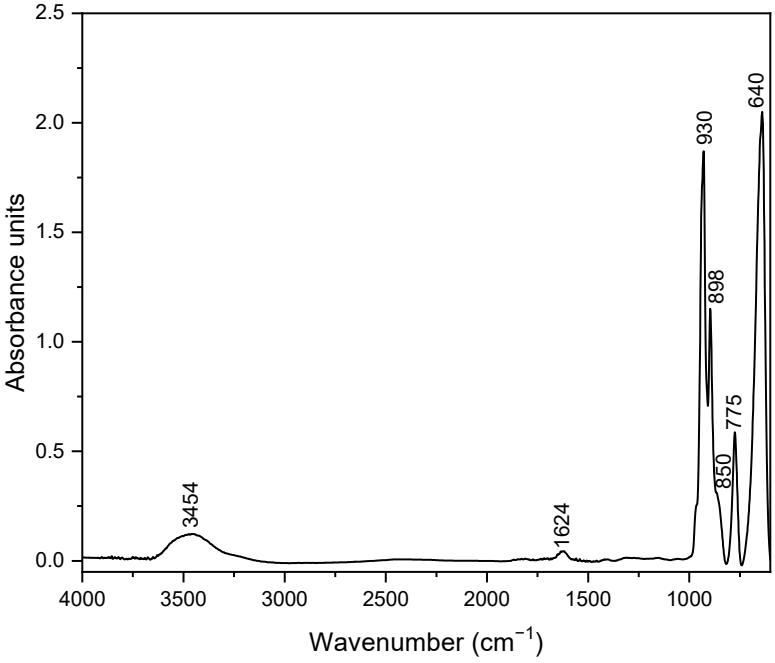

Figure 2. FTIR spectrum of the α-$AgVO_3$ nanowires.

As seen from the figure, the presence of specific characteristic bands accompanied by vibrational groups is indicated. Firstly, the bands between 3454 and 1624 cm^{-1} correspond to the stretching and bending vibration of surface hydroxyl groups (–OH) and water molecules [35]. Further, the FTIR spectrum reveals the presence of distinct bands as follows: a band at 930 cm^{-1}, which corresponds to the symmetric stretching vibrations of VO_3 and the V=O double bond, at 898 cm^{-1}, a band corresponds to V=O stretching, the broad band around 850 cm^{-1} linked to both the V-O stretching vibration and the stretching vibration mode of the Ag-O-V bond [36,37], the band at 775 cm^{-1}, which could be likely assigned to the antisymmetric stretching vibrations of VO_3, and the band at 640 cm^{-1} associated with the symmetric and asymmetric stretching modes of V–O–V [38,39].

The morphology of the prepared α-$AgVO_3$ has been analyzed by SEM/EDS and TEM. The SEM images of the prepared $AgVO_3$ are shown in Figure 3a–d. The SEM micrographs of the synthesized sample revealed that the silver vanadate in the form of nanowires presented dimensions at nanometric and micrometric scales for diameter and length, respectively.

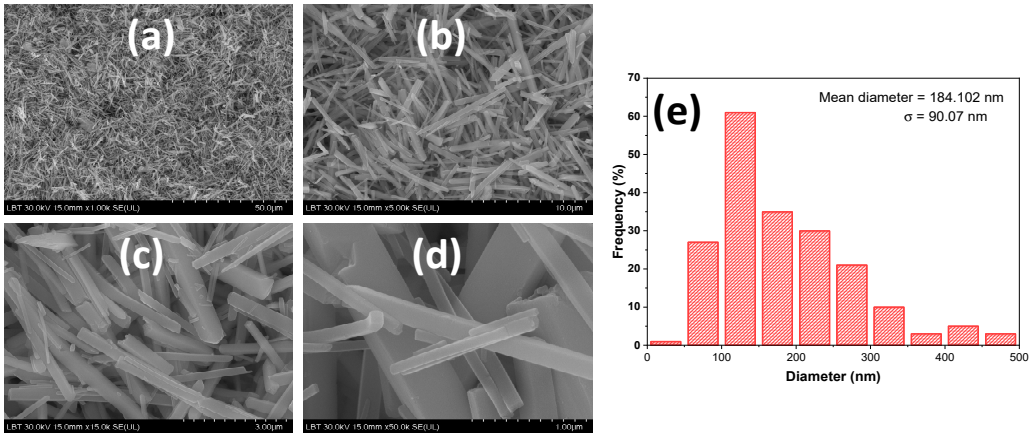

Figure 3. SEM images of α-$AgVO_3$ at different magnifications: (**a**) ×1.00 k, (**b**) ×5.00 k, (**c**) ×15.0 k, and (**d**) ×50.0 k, and (**e**) diameter distribution histogram of nanowires from image (**b**).

The diameters of the nanowires of the silver vanadate were determined from the SEM micrograph (Figure 3b) using ImageJ software, with the results shown in Figure 3e. A large number of nanowires (~200) were considered to build the distribution histogram and calculate the mean diameter. The histogram of the sample presented an asymmetric nanowire diameter distribution with the majority situated between 50 and 150 nm. The calculated mean diameter value was 184.102 nm.

The EDS results indicate that the sample contains only Ag, V, and O, as shown in Figure 4a,b. Further quantitative analysis reveals that the atomic ratio of Ag/V/O is about 1:1:3, suggesting that the sample is stoichiometric and consistent with the XRPD results. To further evaluate the content of Ag, V, and O in the $AgVO_3$ sample, elemental mapping was conducted. The elemental mapping micrographs (Figure 4c–f) confirm that the elements are uniformly distributed in the sample, with silver, vanadium, and oxygen showing homogeneous distribution throughout the imaged area.

The formation of nanowires was further confirmed by the TEM images (Figure 5). As is visible from the TEM image, the surface of the nanowires is coated with metallic semispherical silver particles that can maintain a high contact surface with microorganisms, in agreement with the research previously reported by Ferreira et al. [19].

The prevalence of polymorphism in $AgVO_3$ is a determinant of the varied properties for each compound. It is well known that the properties of $AgVO_3$ greatly depend on the synthesis methods, crystal structure, and hierarchical morphology. Typically, α-$AgVO_3$ and β-$AgVO_3$ exhibit one-dimensional morphologies and can be observed in the form of nanowires, nanorods, or nanotubes [40].

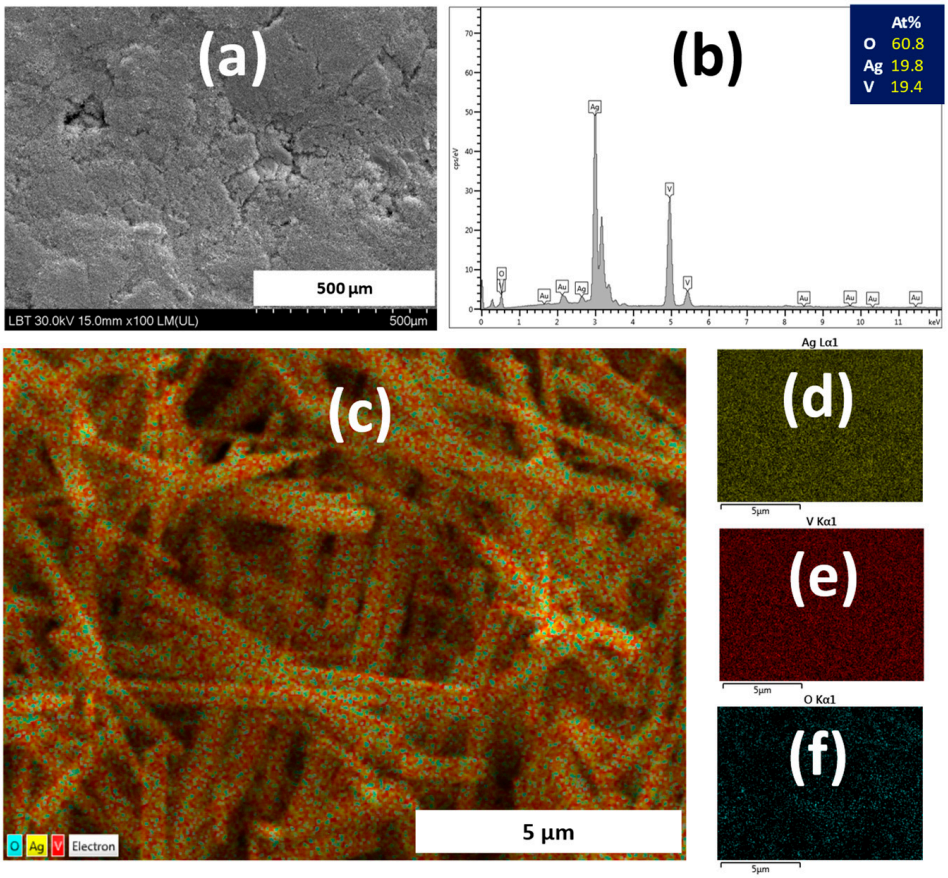

Figure 4. (**a**) SEM image at ×100 LM magnification, (**b**) corresponding EDS spectrum, and (**c**–**f**) SEM/EDS elemental mapping of the $AgVO_3$ sample. In the elemental mapping images, the assignment of color for each element is the following: yellow for Ag, red for V, and blue for O, respectively.

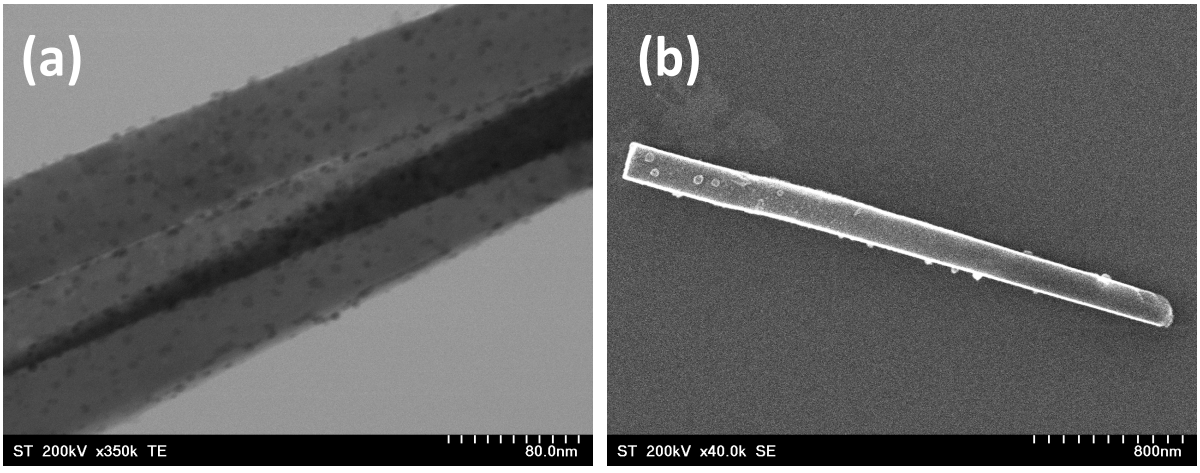

Figure 5. TEM images of $AgVO_3$ at (**a**) ×350 k and (**b**) ×40.0 k magnifications.

There are few studies regarding the morphology of α-$AgVO_3$, which is a metastable phase. Alves da Silva Pimentela et al. synthesized α-$AgVO_3$ microcrystals using the co-precipitation method at three different temperatures (10 °C, 20 °C, and 30 °C) [29]. Microcrystals synthetized at 10 °C showed microrods of α-$AgVO_3$ and well-defined faces. Increasing the temperature at 20 °C leads to a direct self-assembly of nanorods to form urchin-like microspheres. Further, at 30 °C, the microcrystals of α-$AgVO_3$ show predominantly urchin-like morphologies. In addition, the authors revealed that α-$AgVO_3$

microcrystals have antifungal activity, with the obtained MIC and MFC values demonstrating that they are not cytotoxic against keratinocyte cells, regardless of morphological variations on the microcrystals. However, they exhibited fungistatic and fungicidal activity against *C. albicans*. Despite having different morphologies, all the microcrystals showed the same values of MIC and MFC (3.9 μg/mL and 15.62 μg/mL, respectively) [29].

Conversely, most studies from the literature focused on β-$AgVO_3$, the stable polymorph phase. In a comparative study, using the synthesis of β-$AgVO_3$ nanowires by two different methods, precipitation and hydrothermal, crystals with different shapes are revealed [40]. Samples prepared by precipitation were constituted of particles of irregular shape with some rodlike structures with different diameters and lengths, whereas the sample obtained by the hydrothermal method produced samples with one-dimensional morphology, uniform and homogeneous wirelike structures, without the presence of particles with other shapes, with a length of several tens of micrometers. Moreover, the diameters of the nanowires were depending on the molar ratio of Ag/V used for the preparation, 1/1 and 2:1. At a low molar ratio, the nanowires present a diameter of around 60 to 95 nm, whereas at a high molar ratio, most of the nanowires have smaller diameters, between 45 and 70 nm. So, synthesis of β-$AgVO_3$ nanowires performed with a higher Ag/V ratio produced β-$AgVO_3$ nanowires with a narrow diameter distribution and fewer aggregates [40]. In the study of Baptista et al., a monophasic, needle-shaped, and nanometric β-$AgVO_3$ powder was successfully synthesized by a simple hydrothermal route. They identified crystals with an average length of less than 1.5–2 μm and an acicular morphology with a high aspect ratio of 4:1. Moreover, it has been demonstrated that incorporating an antibacterial nanoceramic ($AgVO_3$) into a commercial restorative dental glass–ceramic (IPS d.SIGN) imparts antibacterial properties, requiring a minimum addition of 2 wt% of β-$AgVO_3$. This nanomaterial can be readily synthesized via a simple route. Ferreira et al. conducted a study that indicated that the introduction of β-$AgVO_3$ nanowires coated with semispherical metallic silver nanoparticles, prepared via a precipitation method, demonstrated antimicrobial efficacy across all concentrations (2.5%, 5%, and 10%) when incorporated into dental porcelain. The study also found that this incorporation did not affect the Vickers microhardness [19]. De Castro et al. developed nanostructured silver vanadate with acicular morphology, featuring an average diameter of 150 nm and length in the micrometer range, through a precipitation reaction. Their research substantiated the antibacterial effects in inhibiting biofilm formation by major microorganisms associated with dental prostheses, utilizing PMMA acrylic resins incorporating 0–10% wt.% of β-$AgVO_3$ [25].

3.2. Characterization of Dental Porcelain

Figure 6 shows the XRPD patterns of the dental porcelain samples after sintering at 1300 °C for 1 h. The major crystalline phase quartz (Q), which is dispersed in the vitreous phase, was identified by XRPD in the samples. At a sintering temperature of 1300 °C, the feldspar melted completely and its diffractogram showed a broad band associated with the amorphous phase, as indicated in the XRPD patterns. Moreover, the quartz has transformed from the α phase to the β phase, and these two phases exhibited nearly identical peaks in the XRPD diffractograms.

The dental porcelain samples with 0, 1, 3, and 5 wt.% $AgVO_3$ addition were further examined by FTIR spectroscopy in the spectral region from 4000 to 600 cm^{-1} with the spectral data displayed in Figure 7. The band at 781 cm^{-1} and the very intense one at 1068 cm^{-1} are characteristic of the symmetric and asymmetric stretching vibrations of the Si-O-Si bonds. Our results agree with the results previously reported, which identified absorption bands ranging from 400 to 1400 cm^{-1} associated with the quartz bending band [41,42]. As is known, the bands between 1070 and 1120 cm^{-1} could be assigned to the vibrations of the Si-O-Si bond, which appear in the spectrum of quartz, but also in some silicates where the SiO_4 tetrahedral is linked together by oxygen bridges. Further, the band around 1625 cm^{-1} is attributed to the bending vibrational mode of the H-O-H bonds

corresponding to the adsorbed water molecules, and the broad absorption band with the maximum at 3455 cm^{-1} is attributed to the stretching vibrations of the bond O-H from the hydroxyl groups, which are present on the surface of the material [43,44].

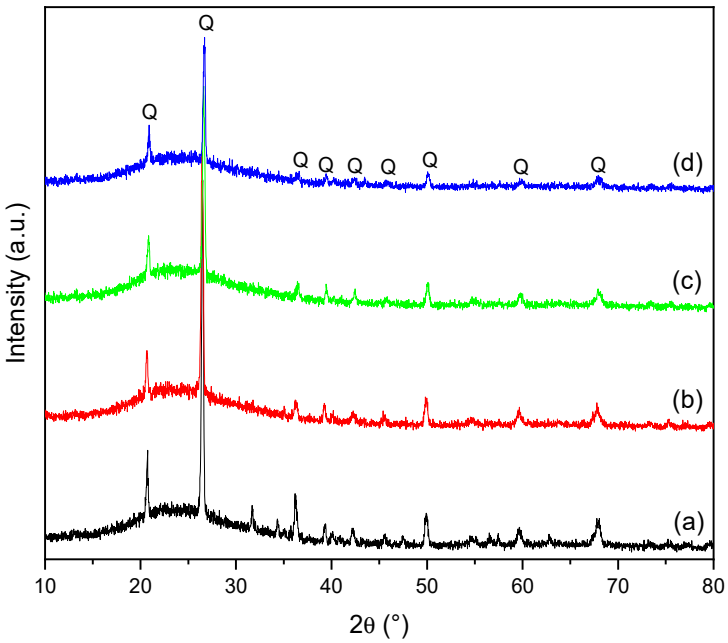

Figure 6. XRPD patterns of DP with (**a**) 0, (**b**) 1, (**c**) 3, and (**d**) 5 wt% α-$AgVO_3$ addition, sintered at 1300 °C (Q-quartz).

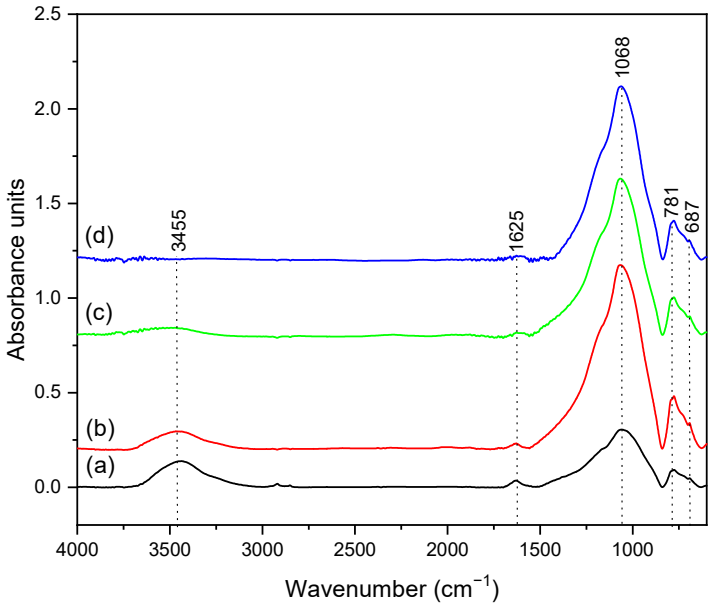

Figure 7. FTIR spectra of DP with (**a**) 0, (**b**) 1, (**c**) 3, and (**d**) 5 wt.% of α-$AgVO_3$ addition, sintered at 1300 °C.

The SEM/EDX morphology and elemental compositions of the prepared DP crystals are presented in Figure 8. As seen from the images, the micrographs show the formation of crystals of different sizes and shapes. The quartz was identified as a major phase, in addition to the amorphous phase. The main raw material used to obtain the DP was the feldspar. The quartz crystals were added as the main source of silica with its role in promoting the reinforcement of the ceramic structure [40]. Dental porcelain materials are characteristically sintered by a viscous flow, formed at different temperatures. At this point, quartz grains

remain as crystals surrounded by fusible compounds. A multiphase translucent material is formed at room temperature, corresponding to a ceramic material with a dispersed, crystalline phase and a continuous, amorphous phase, originating from feldspar and other low-melting impurities in the raw materials [45]. Typical surface microstructures for quartz grains with sharp angular features, in agreement with the XRPD data, are displayed on the SEM images. Most importantly, the addition of $AgNO_3$ has no morphological effect on the crystals. The EDS analyses confirmed the presence of both dopant Ag and V ions in crystals, as well as other elements derived from the DP composition. The EDS detected an increasing weight percentage of Ag, which corresponds to the increased amount of $AgVO_3$ on the DP samples.

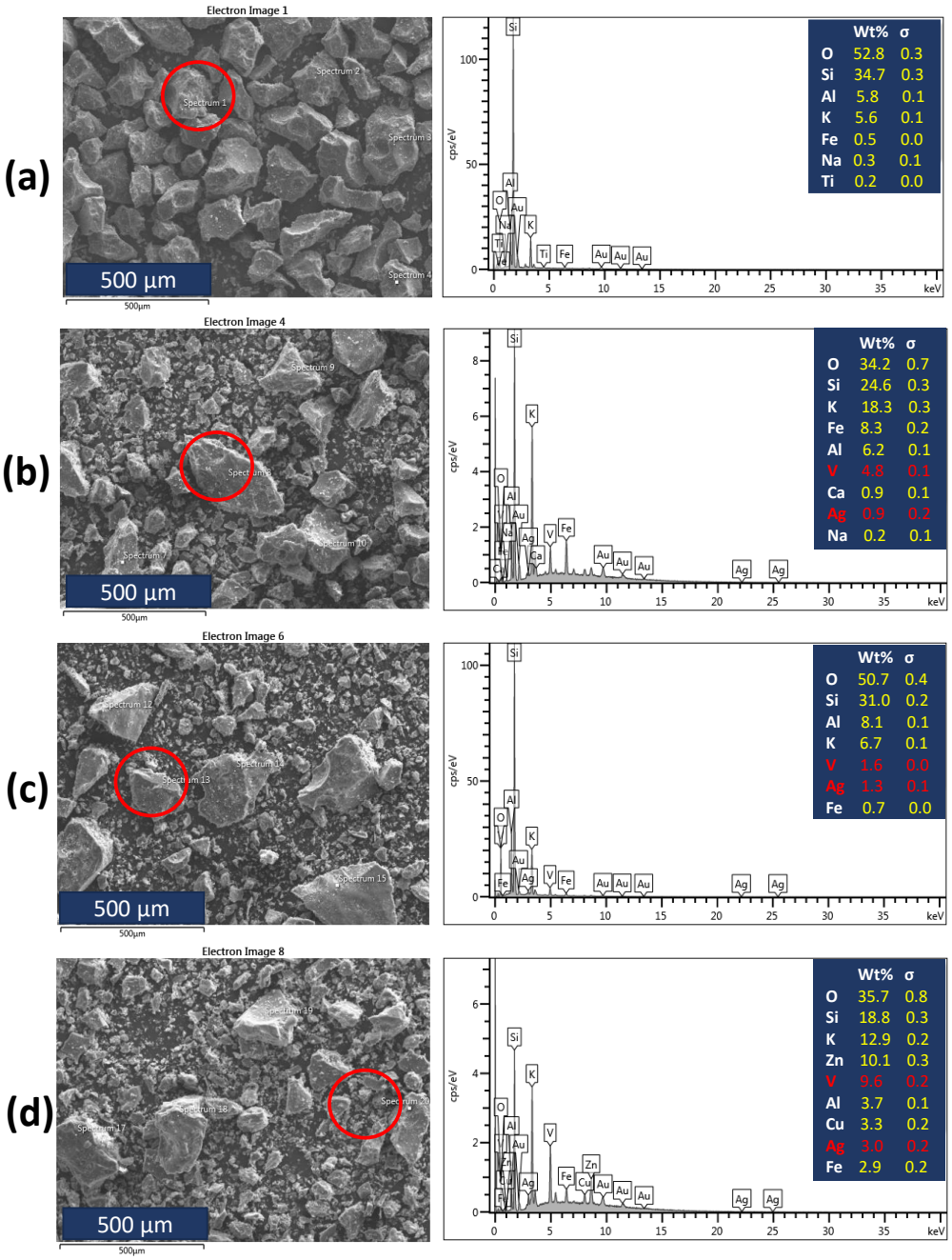

Figure 8. SEM (**left**) and EDX (**right**) analysis realized for the DP samples, with (**a**) 0, (**b**) 1, (**c**) 3, and (**d**) 5 wt.% addition of α-$AgVO_3$. The surface of each composition was analyzed by EDX with circles indicating the chosen area.

Following the SEM/EDS analysis, the morphology and elemental compositions of the prepared DP crystals are shown in Figure 8.

Considering the results of these preliminary studies, further studies are required to clarify the effect and potential impact of α-$AgVO_3$ addition on the antibacterial properties of the prepared dental porcelain.

4. Conclusions

Silver-containing microcrystals have been extensively studied due to their excellent properties, especially concerning biocompatibility relative to silver-containing nanoparticles. In addition to the well-studied β-$AgVO_3$, the α-$AgVO_3$ also demonstrates efficiency for a range of pathogenic bacteria, making it an interesting antibacterial agent for biomedical applications. In this study, nanostructured α-$AgVO_3$ was synthesized through a precipitation reaction between $AgNO_3$ and NH_4VO_3. Further, different amounts of 1, 3, and 5 wt.% α-$AgVO_3$ were added to a new dental porcelain (DP) mass prepared from natural raw materials, sintered at 1300 °C. The structural and morphological properties of α-$AgVO_3$ and DP were investigated by XRPD, FTIR, and SEM/EDS. The results showed the formation of α-$AgVO_3$ nanowires coated with metallic silver nanoparticles. It has been found that the incorporation of α-$AgVO_3$ did not lead to a difference in the structural and morphological properties of the prepared DP. Further studies are required to elucidate the effectiveness of α-$AgVO_3$ as a candidate for potentially improving the antibacterial properties of the ceramic dental material.

Author Contributions: Conceptualization, L.B.; methodology, L.B., M.M.-P. and T.L.; software, L.B. and M.M.-P.; validation, L.B. and M.M.-P.; investigation, B.E.S., M.M.-P., L.B.-T. and T.L.; writing—original draft preparation, L.B., B.E.S. and M.M.-P.; writing—review and editing, L.B., B.E.S. and M.M.-P.; visualization, B.E.S., L.B., M.M.-P. and T.L.; supervision, L.B. All authors have read and agreed to the published version of the manuscript.

Funding: This research received no external funding.

Institutional Review Board Statement: Not applicable.

Informed Consent Statement: Not applicable.

Data Availability Statement: The data presented in this study are available on request from the corresponding author due to privacy.

Conflicts of Interest: The authors declare no conflicts of interest.

References

1. National Institute of Biomedical Imaging and Bioengineering. Available online: https://www.nibib.nih.gov/science-education/science-topics/biomaterials (accessed on 27 May 2024).
2. Kaur, G. *Clinical Applications of Biomaterials. State-of-the-Art Progress, Trends, and Novel Approaches*, 1st ed.; Springer: Cham, Switzerland, 2017; pp. 1–26.
3. Wong, J.Y.; Bronzino, J.D. *Biomaterials*; CRC Press: Boca Raton, FL, USA, 2016; pp. 38–71.
4. Bharadwaj, A. An Overview on Biomaterials and Its Applications in Medical Science. *IOP Conf. Ser. Mater. Sci. Eng.* **2021**, *1116*, 012178. [CrossRef]
5. Hench, L.L. Bioceramics: From Concept to Clinic. *J. Am. Ceram. Soc.* **1991**, *74*, 1487–1510. [CrossRef]
6. Buxbaum, E. Bond Properties. In *Biophysical Chemistry of Proteins*; Springer: Boston, MA, USA, 2011; p. 453.
7. Debelian, G.; Trope, M. The Use of Premixed Bioceramic Materials in Endodontics. *G. Ital. Endod.* **2016**, *30*, 70–80. [CrossRef]
8. Keane, T.J.; Badylak, S.F. Biomaterials for Tissue Engineering Applications. *Semin. Pediatr. Surg.* **2014**, *23*, 112–118. [CrossRef] [PubMed]
9. Zheng, L.W.; Wang, J.Y.; Yu, R.Q. Biomaterials in Dentistry. *Encycl. Biomed. Eng.* **2019**, *1–3*, 278–288.
10. Sarikaya, I.; Güler, A.U. Effects of Different Polishing Techniques on the Surface Roughness of Dental Porcelains. *J. Appl. Oral Sci.* **2010**, *18*, 10–16. [CrossRef] [PubMed]
11. Jones, D.W. Ceramic Biomaterials. *Key Eng. Mater.* **1996**, *122–124*, 345–386. [CrossRef]
12. Anusavice, K.J.; Shen, C.; Rawls, H.R. *Phillips' Science of Dental Materials*; Elsevier: St. Louis, MO, USA, 2013; pp. 1–538.
13. Sakaguchi, R.L.; Powers, J.M. *Craig's Restorative Dental Materials*, 13th ed.; Elsevier: Philadelphia, PA, USA, 2012; pp. 135–146.

14. Naert, I. 7.24 Materials in Fixed Prosthodontics for Indirect Dental Restorations. In *Comprehensive Biomaterials II*; Ducheyne, P., Ed.; Elsevier: London, UK, 2017; pp. 467–481.
15. Van Noort, R.; Barbour, M.E. *Introduction to Dental Materials*, 5th ed.; Elsevier: London, UK, 2013; pp. 1–15.
16. El-Meliegy, E.; van Noort, R. History, Market and Classification of Bioceramics. In *Glasses and Glass Ceramics for Medical Applications*; Springer: New York, NY, USA, 2012; pp. 3–17.
17. Durán, N.; Marcato, P.; De Conti, R.; Alves, O.; Costa, F.; Brocchi, M. Potential Use of Silver Nanoparticles on Pathogenic Bacteria, Their Toxicity and Possible Mechanisms of Action. *J. Braz. Chem. Soc.* **2010**, *21*, 949–959. [CrossRef]
18. Uehara, L.M.; Ferreira, I.; Botelho, A.L.; Valente, M.L.D.C.; Reis, A.C.D. Influence of β-$AgVO_3$ Nanomaterial Incorporation on Mechanical and Microbiological Properties of Dental Porcelain. *Dent. Mater.* **2022**, *38*, e174–e180. [CrossRef]
19. Ferreira, I.; Vidal, C.L.; Botelho, A.L.; Ferreira, P.S.; Valente, M.L.C.; Schiavon, M.A.; Alves, O.L.; dos Reis, A.C. Effect of Nanomaterial Incorporation on the Mechanical and Microbiological Properties of Dental Porcelain. *J. Prosthet. Dent.* **2020**, *123*, 529.e1–529.e5. [CrossRef]
20. Vidal, L.; Ferreira, I.; Ferreira, P.; Valente, M.; Teixeira, M.; Reis, A. Incorporation of Hybrid Nanomaterial in Dental Porcelains: Antimicrobial, Chemical, and Mechanical Properties. *Antibiotics* **2021**, *10*, 98. [CrossRef] [PubMed]
21. Fernandez, C.C.; Sokolonski, A.R.; Fonseca, M.S.; Stanisic, D.; Araújo, D.B.; Azevedo, V.; Portela, R.D.; Tasic, L. Applications of Silver Nanoparticles in Dentistry: Advances and Technological Innovation. *Int. J. Mol. Sci.* **2021**, *22*, 2485. [CrossRef] [PubMed]
22. Holtz, R.D.; Filho, A.G.S.; Brocchi, M.; Durán, N.; Alves, O.L. Development of Nanostructured Silver Vanadates Decorated with Silver Nanoparticles as a Novel Antibacterial Agent. *Nanotechnology* **2010**, *21*, 185102. [CrossRef] [PubMed]
23. Balan, L.; Malval, J.P.; Schneider, R.; Burget, D. Silver Nanoparticles: New Synthesis, Characterization and Photophysical Properties. *Mater. Chem. Phys.* **2007**, *104*, 417–421. [CrossRef]
24. Baptista, I.O.; Alves, M.F.R.P.; Ferreira, S.; Santos, C.; Vieira, S.I.; Fernandes, M.H.V. Antibacterial activity improvement of dental glass-ceramic by incorporation of $AgVO_3$ nanoparticles. *Dent. Mater.* **2022**, *38*, 1679–1688. [CrossRef] [PubMed]
25. De Castro, D.T.; Valente, M.L.C.; Da Silva, C.H.L.; Watanabe, E.; Siqueira, R.L.; Schiavon, M.A.; Alves, O.L.; dos Reis, A.C. Evaluation of Antibiofilm and Mechanical Properties of New Nanocomposites Based on Acrylic Resins and Silver Vanadate Nanoparticles. *Arch. Oral Biol.* **2016**, *67*, 46–53. [CrossRef] [PubMed]
26. Assis, M.; da Silva, J.S.; Gonçalves, M.O.; de Almeida Rodolpho, J.M.; de Lima Fragelli, B.D.; Corte, A.B.P.; Ribeiro, L.K.; Teodoro, M.D.; de Freitas Anibal, F.; de Sousa, C.P.; et al. Bactericidal Activity of $Ag_4V_2O_7$/β-$AgVO_3$ Heterostructures against Antibiotic-Resistant Klebsiella Pneumoniae. *Biomater. Adv.* **2022**, *141*, 213097. [CrossRef] [PubMed]
27. de Campos, M.R.; Botelho, A.L.; Dos Reis, A.C. Nanostructured silver vanadate decorated with silver particles and their applicability in dental materials: A scope review. *Heliyon* **2021**, *7*, e07168. [CrossRef] [PubMed]
28. Monteiro, A.; Dias Holtz, R.; Carneiro, F.; Zanini, M.; De Sousa, M. Nano Silver Vanadate $AgVO_3$: Synthesis, New Functionalities and Applications. *Chem. Rec.* **2018**, *18*, 973–985. [CrossRef]
29. Alves da Silva Pimentel, B.N.; de Foggi, C.C.; Barbugli, P.A.; de Oliveira, R.C.; de Avila, E.D.; Longo, E.; Vergani, C.E. Antifungal activity and biocompatibility of α-$AgVO_3$ microcrystals: A promising material against oral Candida disease. *Mater. Sci. Eng. C* **2020**, *108*, 110405. [CrossRef]
30. Ferreira, I.; Alves, O.L.; Schiavon, M.A.; dos Reis, A.C. Influence of incorporation of nanostructured silver vanadate decorated with silver nanoparticles on roughness, microhardness, and color change of pit and fissure sealants. *Heliyon* **2024**, *10*, e25525. [CrossRef] [PubMed]
31. Alvim, G.C.; Oliveira, V.d.C.; dos Reis, A.C.; Schiavon, M.A.; Pinto, M.R.; da Silva, M.V.; Lepri, C.P.; de Castro, D.T. Effect of silver vanadate on the antibiofilm, adhesion and biocompatibility properties of denture adhesive. In *Future Microbiology*; Taylor and Francis: Oxfordshire, UK, 2024; pp. 1–11.
32. Kreve, S.; Oliveira, V.C.; Bachmann, L.; Alves, O.L. Influence of $AgVO_3$ Incorporation on Antimicrobial Properties, Hardness, Roughness and Adhesion of a Soft Denture Liner. *Sci. Rep.* **2019**, *9*, 11889. [CrossRef] [PubMed]
33. de Oliveira, R.C.; de Foggi, C.C.; Mondego Teixeira, M.; Penha da Silva, M.D.; Assis, M.; Francisco, E.M.; Alves da Silva Pimentel, B.N.; dos Santos Pereira, P.F.; Vergani, C.E.; Machado, A.L.; et al. Mechanism of Antibacterial Activity via Morphology Change of α-$AgVO_3$: Theoretical and Experimental Insights. *ACS Appl. Mater. Interfaces* **2017**, *9*, 11472–11481. [CrossRef] [PubMed]
34. Kittaka, S.; Matsuno, K.; Akashi, H. Crystal structure of alpha-$AgVO_3$ and phase relation of $AgVO_3$. *J. Solid State Chem.* **1999**, *142*, 360–367. [CrossRef]
35. Esmaeili, E.; Salavati-Niasari, M.; Mohandes, F. Modified Single-Phase Hematite Nanoparticles via a Facile Approach for Large-Scale Synthesis. *Chem. Eng. J.* **2011**, *170*, 278–285. [CrossRef]
36. Liu, H.; Tang, D. Synthesis of ZnV_2O_6 Powder and Its Cathodic Performance for Lithium Secondary Battery. *Mater. Chem. Phys.* **2009**, *114*, 656–659. [CrossRef]
37. Wu, J.; Li, L.; Li, X.; Min, X. A novel 2D graphene oxide modified α-$AgVO_3$ nanorods: Design, fabrication, and enhanced visible-light photocatalytic performance. *J. Adv. Ceram.* **2022**, *11*, 308–320. [CrossRef]
38. Vilela Teixeira, A.B.; Larissa Vidal, C.; Albiasetti, T.; Tornavoi De Castro, D.; Cândido Dos Reis, A. Influence of Adding Nanoparticles of Silver Vanadate on Antibacterial Effect and Physicochemical Properties of Endodontic Sealers. *Iran. Endod. J.* **2019**, *14*, 7–13. [PubMed]
39. da Silva, J.S.; Machado, T.R.; Trench, A.B.; Silva, A.D.; Teodoro, V.; Vieira, P.C.; Martins, T.A.; Longo, E. Enhanced photocatalytic and antifungal activity of hydroxyapatite/α-$AgVO_3$ composites. *Mat. Chem. Phys.* **2020**, *252*, 123294. [CrossRef]

40. de Menezes, B.R.C.; Ribas, R.G.; Schatkoski, V.M.; do Amaral Montanheiro, T.L.; Koga-Ito, C.Y.; Thim, G.P. Synthesis of β-$AgVO_3$ nanowires by hydrothermal and precipitation routes: A comparative study. *SN Appl. Sci.* **2019**, *1*, 1327. [CrossRef]
41. Harabi, A.; Guerfa, F.; Harabi, E.; Benhassine, M.T.; Foughali, L.; Zaiou, S. Preparation and Characterization of New Dental Porcelains, Using K-Feldspar and Quartz Raw Materials. Effect of B_2O_3 Additions on Sintering and Mechanical Properties. *Mater. Sci. Eng. C* **2016**, *65*, 33–42. [CrossRef] [PubMed]
42. Kieffer, S. Thermodynamics and Lattice Vibrations of Minerals: 2. Vibrational Characteristics of Silicates. *Rev. Geophys. Space Phys.* **1979**, *17*, 20–34. [CrossRef]
43. Kooli, F.; Yan, L.; Tan, S.; Zheng, J. Organoclays from Alkaline-Treated Acid-Activated Clays: Properties and Thermal Stability. *J. Therm. Anal. Calorim.* **2014**, *115*, 1465–1475. [CrossRef]
44. Komadel, P. Chemically Modified Smectites. *Clay Miner.* **2003**, *38*, 127–138. [CrossRef]
45. Lawson, N.C.; Burgess, J.O. Dental ceramics: A current review. *Comp. Cont. Educ. Dent.* **2014**, *35*, 161–166.